



Explicit- and Implicit-Solvent Simulations of Micellization in Surfactant Solutions

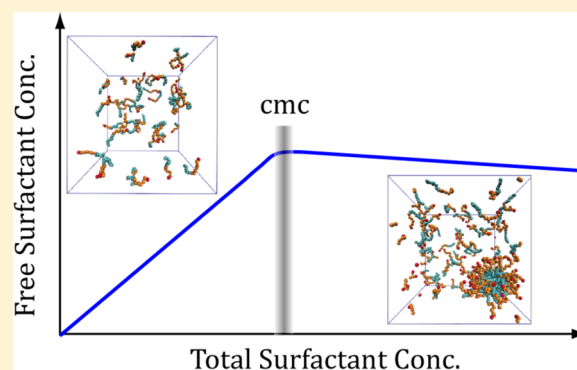
Arben Jusufi[†] and Athanassios Z. Panagiotopoulos^{*,‡}

[†]Department of Chemistry, College of Staten Island and Graduate Center, City University of New York, Staten Island, New York 10314, United States

[‡]Department of Chemical and Biological Engineering, Princeton University, Princeton, New Jersey 08544, United States

ABSTRACT: In this article, we focus on simulation methodologies to obtain the critical micelle concentration (cmc) and equilibrium distribution of aggregate sizes in dilute surfactant solutions. Even though it is now relatively easy to obtain micellar aggregates in simulations starting from a fully dispersed state, several major challenges remain. In particular, the characteristic times of micelle reorganization and transfer of monomers from micelles to free solution for most systems of practical interest exceed currently accessible molecular dynamics time scales for atomistic surfactant models in explicit solvent. In addition, it is impractical to simulate highly dilute systems near the cmc. We have demonstrated a strong dependence of the free surfactant concentration (frequently, but incorrectly, taken to represent the cmc in simulations) on the overall

concentration for ionic surfactants. We have presented a theoretical framework for making the necessary extrapolations to the cmc. We find that currently available atomistic force fields systematically underpredict experimental cmc's, pointing to the need for the development of improved models. For strongly micellizing systems that exhibit strong hysteresis, implicit-solvent grand canonical Monte Carlo simulations represent an appealing alternative to atomistic or coarse-grained, explicit-solvent simulations. We summarize an approach that can be used to obtain quantitative, transferrable effective interactions and illustrate how this grand canonical approach can be used to interpret experimental scattering results.



INTRODUCTION

The formation of micellar aggregates in surfactant solutions is critical to many applications in nanotechnology, detergency, and catalysis; the process is driven by physicochemical forces similar to those leading to protein folding, aggregation, and biological membrane self-assembly. Because of its importance, micellization in surfactant solutions has been extensively studied experimentally, theoretically, and by computer simulations. Micellization takes place in dilute solutions; the critical micelle concentration above which aggregates are observed depends on the molecular character of the surfactant and solvent, the temperature, and the presence of added salt or other solutes. Micellar aggregates composed of low-molecular-mass surfactants are typically stable over time scales of microseconds or above and contain from a few dozen to hundreds of surfactant molecules. These characteristics of the micellization process render equilibrium simulations of spontaneous self-assembly quite challenging, as detailed in the next section.

In molecular-simulation based studies of micellization in dilute surfactant solutions, several key questions need to be addressed, as follows: Given a certain surfactant or mixture of surfactants and a specific solvent environment (e.g., water), what is the critical micelle concentration (cmc), and how does it vary with temperature and salt concentration? What are the

size, shape, and structure of micellar aggregates that form at concentrations near the cmc, and what are their size and shape polydispersities? How do solutes partition between free solution and the micellar interior?

The main objective of this article is to survey two recent developments that have provided pathways for the molecular description of micellization in dilute surfactant solutions, addressing the questions above. The first approach, applicable to explicit-solvent models, involves long molecular dynamics simulations of spontaneous self-assembly at elevated concentrations, with subsequent extrapolation to conditions relevant to the cmc. The second approach utilizes implicit-solvent models in which effective interactions between surfactant molecules are obtained to represent the solvent; the approach is based on grand canonical Monte Carlo simulations that connect the free energy of aggregates to that of free surfactants. A recent focused review by one of us¹ also covers these two developments, but from a somewhat different viewpoint. Comprehensive reviews of computer simulations of surfactant systems are also available.^{2,3} We restrict our attention to dilute systems for which micellization is driven entirely by

Received: June 6, 2014

Revised: August 28, 2014

Published: September 16, 2014



thermodynamic equilibrium considerations, excluding non-equilibrium aggregation that can occur for long block copolymers even over experimental time scales. Micellar shape transitions and liquid-crystalline mesophases that form in concentrated surfactant solutions are outside the scope of the present survey.

The structure of this article is as follows. The next section describes the main challenges for molecular-based simulations of surfactant self-assembly. This is followed by a section on the relationship between observed free surfactant concentration and the critical micelle concentration; this dependence has been neglected in most prior simulation studies of self-assembly, leading to potentially inaccurate results. The two main sections that follow cover explicit- and implicit-solvent recent studies. The article concludes with a summary of the main unresolved questions, focusing in particular on the issue of force-field optimization to achieve quantitative agreement with experiments and allow for predictive modeling of systems for which experimental data are not available.

■ TIME AND LENGTH SCALES

In Figure 1, we show a schematic illustration of “free” versus total surfactant concentration during micellization. The total

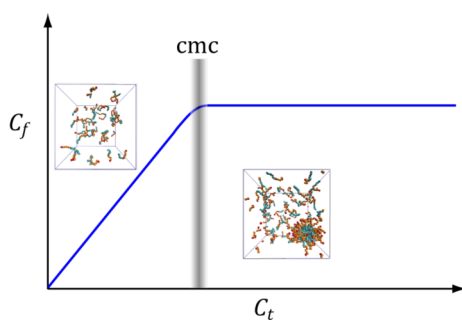


Figure 1. Schematic illustration of free surfactant concentration, C_f , versus total surfactant concentration, C_t , for a micellizing system.

concentration, C_t , is the macroscopic amount of surfactant in the system, a directly controlled quantity in both experiments and simulations. The free surfactant concentration, C_f , needs to be operationally defined; it represents surfactant monomers and submicellar aggregates. The surfactant concentration is usually measured in units of moles of solute per liter of solution, $1 \text{ M} \equiv 1 \text{ mol/L}$. In this classic picture, all surfactant molecules exist as kinetically independent entities in solution and are not part of long-lived micellar aggregates, up to the first cmc. The cmc is shown as a gray band because micellization is not a thermodynamic phase transition; different methods of inferring the existence of aggregates give slightly different results for the cmc. Above the cmc, a common assumption is that the free surfactant concentration remains constant because any added molecules end up in micelles rather than free in solution.⁴ There is, of course, a continuous, dynamic exchange of molecules between micelles and free solution at all concentrations, but the average number of molecules found in aggregates of any specific size remains constant at equilibrium. The free surfactant concentration for a micellizing system is often taken as a proxy for the cmc itself, especially in simulations, which are much easier to perform at overall loadings much above the cmc. As we will shall discuss in the next section, in contrast to this idealized picture, the free

surfactant concentration C_f does not remain constant above the cmc, especially for ionic surfactants.

The cmc of a commonly studied ionic surfactant, sodium dodecyl sulfate (SDS), is approximately 8 mM at room temperature.⁵ A typical micellar aggregate near the cmc for this system contains around 60 surfactant molecules.⁶ These two facts imply that a simulation study of SDS that includes a few hundred surfactant molecules (in order to allow the formation of several micellar aggregates) also needs to incorporate millions of water molecules if it is to be at concentrations dilute enough to be near the cmc. Thus, the simulation length scales required for modeling such low concentrations are tens of nanometers. Such large systems require significantly more computational resources relative to more commonly simulated systems of a few thousand interaction centers. Time scales for the exchange of monomers between the micellar interior and free solution are on the order of microseconds.⁷ Clearly, atomistic, explicit-solvent simulations of such systems for sufficiently long times to allow for the equilibration of the micellar aggregates are currently computationally infeasible. An additional difficulty for ionic surfactants is that the equilibration of the local ionic environment around a micellar aggregate can be quite slow, and the concentration of ions in the vicinity of the headgroups can be quite different than in bulk solution, which in turn poses challenges for simulations that contain only a limited number of ions.

A remedy for the length-scale issue chosen by most simulation work to date is to study concentrations much higher than the cmc, with a corresponding lower ratio of water-to-surfactant molecules. Such simulations can sample trajectories tens or hundreds of nanoseconds long, over which one can observe aggregation starting from a fully dispersed surfactant system⁸ because the nucleation of micellar aggregates is relatively rapid in concentrated solutions. However, achieving true equilibration with respect to the partitioning of surfactant molecules between micelles and free solution, especially with respect to the size distribution of aggregates, is much harder.

An illustration of this point is provided in Figure 2 from explicit-solvent simulations of a coarse-grained model for SDS.⁹ The number of free surfactant molecules in solution, N_f , and the mean aggregate size, $\langle M \rangle$, are plotted as functions of time for three total surfactant concentrations, all of which are significantly above the cmc. As stated in the previous paragraph, the free surfactant concentration has commonly been taken to be a measure of the cmc, even though as seen clearly in Figure 2 it varies greatly for the three different overall surfactant concentrations studied (top graph). For the more concentrated 1 M system, this quantity requires equilibration times on the order of $0.5 \mu\text{s}$ for the coarse-grained model of ref 9. The mean aggregation number of the micelles (bottom graph) is much slower to equilibrate and still has not reached a fully stationary state even after $6 \mu\text{s}$ for the least-concentrated (130 mM) system. Clearly, accurate (equilibrium) modeling of micelle aggregation numbers and shape transitions, e.g., from spherical to cylindrical micelles, are still beyond the reach of molecular dynamics simulations even for relatively simple low-molecular-mass surfactants. Moreover, determining the cmc's requires a careful consideration of overall surfactant concentration effects, as detailed in the section that follows.

■ DEPENDENCE OF C_f ON C_t

Because the dependence of the free surfactant concentration, C_f , on the total surfactant concentration, C_t , has been

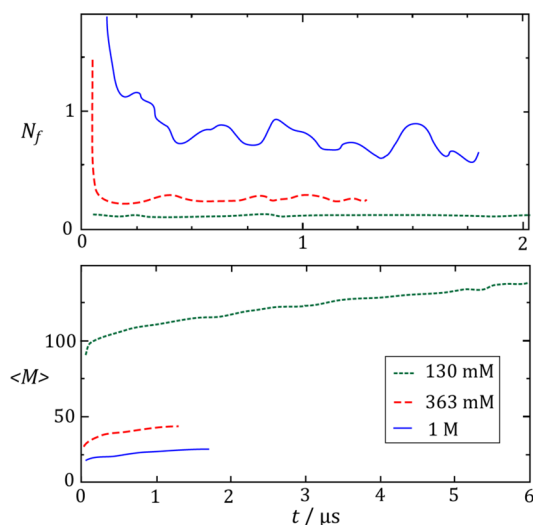


Figure 2. Number of free monomers (top) and mean aggregate size (bottom) as functions of time for a coarse-grained SDS explicit-solvent model.⁹ Solid blue lines are for total surfactant concentration of 1 M, long-dashed red lines are for 363 mM, and short-dashed green lines are for 130 mM. There were 500 total surfactant molecules in the 130 mM system and 1000 in the 363 mM and 1 M systems.

neglected in most prior simulation studies, we present here a summary of the relationships between these quantities for ionic surfactants.^{1,10} For nonionic surfactants, a decrease in the free surfactant concentration has also been observed with overall surfactant loading.¹¹

The total free energy density F of a system containing free monomers, micelles of aggregation number n , and counterions can be written as

$$\beta F = C_n \beta F_n + C_f \beta F_f + \sum_{i=f,n,c} C_i (\ln C_i - 1) \quad (1)$$

where C_f , C_n , and C_c denote the concentrations of free monomers, micelles, and counterions, respectively; F_f and F_n are free energies of surfactants and micelles of size n , respectively, excluding the translational entropy term explicitly represented by the last term summing over all three entities. The inverse thermal energy is given by $\beta = 1/(k_B T)$. Note that eq 1 does not contain the chemical potential term that controls C_t because this term vanishes upon minimization. Minimizing eq 1 with respect to C_f , n , and the fraction of bound counterions α (those associated with micelles) yields three equations that can be solved simultaneously.^{1,10} In performing the differentiations, we ignore micelle solution nonidealities resulting from micelle–micelle and micelle–monomer interactions, an assumption justified given the good agreement of the resulting expressions with simulation and experimental results.^{9,10,12} For C_f , one obtains¹⁰

$$\ln C_f = \frac{1}{1 + \alpha} \times \left[\beta \left(\frac{\Delta G}{n} - x \frac{C_f}{n} \frac{\partial \Delta G}{\partial C_f} \right) - \alpha \ln(1 + (1 - \alpha)x) \right] \quad (2)$$

The dimensionless surfactant concentration parameter is $x = nC_n/C_f = (C_t - C_f)/C_f$. Equation 2 contains free-energy contribution $\Delta G = F_n - nF_f$ that drives self-assembly and has been theoretically evaluated for ionic and nonionic surfactant

micelles.^{13–19} This free-energy contribution is decomposed into an electrostatic and a charge-neutral term such that $\Delta G = \Delta G^{\text{el}} + \Delta G^{\text{ne}}$. For the charge-neutral term, several expressions have been derived for nonionic surfactants.^{14,15,18} We use the expression by Maibaum et al.¹⁸ The electrostatic contribution, ΔG^{el} , accounts for the free-energy cost of charging a spherical micelle of radius R and valency $(1 - \alpha)n$ in an aqueous dielectric medium. Because of counterion association, only a fraction of the charged surfactants contributes to the overall charge of the micelle. The free-energy cost is reduced by eliminating n free monomers and αn counterions of radii r_s and r_c respectively.¹⁷ Overall one obtains

$$\Delta G^{\text{el}} = U((1 - \alpha)n, R) - n[U(-1, r_s) + \alpha U(1, r_c)] \quad (3)$$

where $\beta U(z, r) = z^2 \lambda_B / [2r(1 + \kappa r)]$ is the electrostatic self-energy in the Debye–Hückel approximation,²⁰ with screening length $\kappa = (4\pi \lambda_B (2C_f + (1 - \alpha)x C_f))^{1/2}$. The Bjerrum length is $\lambda_B = 0.72$ nm for water at 298 K.

Equation 2 reduces to a simple expression at the limit of $x \rightarrow 0$. Assuming micelles with sizes of $n \gg 1$, for $x \ll 1$, the last term in eq 2, stemming from counterion entropy, and the term containing $\partial \Delta G / \partial C_f$ vanish. The latter essentially accounts for the change in electrostatic screening with concentration, through $\kappa(C_f)$. As a result, $C_f \rightarrow \text{cmc}$ and eq 2 simplifies to

$$\ln(\text{cmc}) = \frac{\beta \Delta G}{(1 + \alpha)n} \quad (4)$$

This equation relates the cmc to the free-energy difference per particle (monomers and counterions) that are associated with a micelle of aggregate size n , compared to the same number of particles being dispersed in bulk. The number of particles associated with such a micelle is given by the number of surfactants n plus the number of counterions αn . In the opposite limit, $x > 1$, all terms in eq 2 are important, but generally, the counterion entropic term dominates the term $\partial \Delta G / \partial C_f$. Neglecting the latter term allows a transformation of eq 2 into an expression that has been utilized previously by experimentalists to determine free monomer concentrations as a function of total surfactant concentrations for ionic micelles.^{21–23} When eq 4 and the definition $x = (C_t - C_f)/C_f$ are used, eq 2 becomes

$$\ln C_f = (1 + \alpha) \ln(\text{cmc}) - \alpha \ln \left[\frac{(1 - \alpha)(C_t - C_f) + C_f}{1 - \nu C_t} \right] \quad (5)$$

This equation neglects changes in electrostatic screening; surfactant concentration effects are mainly accounted for by changes in the entropy of unbound counterions. Equation 5 also contains a surfactant self-volume correction νC_t (molar volume ν) that is missing from eq 2, although it could be easily included there as well.

Figure 3 shows a comparison of eqs 2 and 5 using length scale parameters appropriate for SDS, $r_s = 0.272$ nm and $r_c = 0.153$ nm, obtained from atomistic simulations.²⁴ The minor discrepancy between the two approaches (solid and dashed lines) is mainly due to the neglect of changes in electrostatic screening. Free monomer data reported in ref 23 that were obtained from eq 5 using an experimental cmc of 8 mM and measured degrees of counterion association α at different values of C_t are also shown.

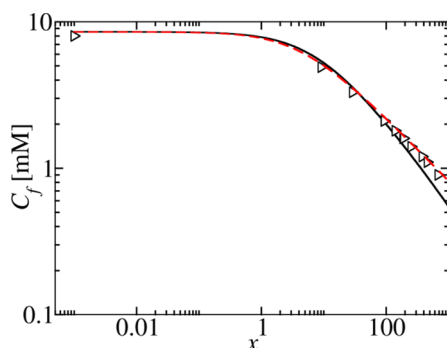


Figure 3. Free surfactant concentration C_f as a function of concentration parameter $x = (C_t - C_f)/C_f$ for SDS. The solid line shows results using eq 2 with model parameters described in the text. The dashed line is obtained from eq 5 using the same parameters. Also shown are results²³ obtained from solving eq 5 using experimental values for the cmc and for degrees of counterion binding α (triangles).

To summarize, eqs 2 and 5 can be used to account for surfactant concentration effects on the free surfactant concentration. The latter equation is an approximation of the first. These expressions open up two possibilities for extrapolating simulation data from high concentrations to the cmc. In the first approach, one performs a single simulation at a high value of $C_t \gg \text{cmc}$ and obtains the free monomer concentration. Then, the theoretical model of eq 2 is used to obtain the cmc. This approach has the advantage of allowing cmc predictions for related surfactants of different alkyl chain length m , for which the parameters of eq 2 change in a known fashion with m .^{1,9,10,18} The second, more direct approach, utilizes eq 5. Here, one performs a series of simulations at different C_t values to obtain C_f and α . Extrapolating the cmc value from eq 5 has been demonstrated recently for an atomistic model of sodium octyl sulfate in explicit water at 298 K,¹² as illustrated in Figure 4.

■ EXPLICIT-SOLVENT SIMULATIONS

Micellization is a phenomenon observed in liquid solutions, with the solvent playing a key role in driving aggregation through favorable (solvophilic) and unfavorable (solvophobic) interactions with segments of the surfactant molecules. The

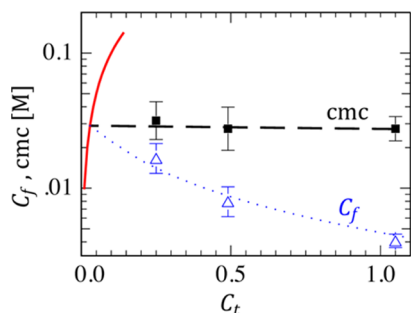


Figure 4. Free surfactant concentration, C_f (blue triangles), and extrapolated cmc (black squares) versus total surfactant concentration, C_t .¹² The solid red line represents a linear relationship of unit slope, $C_f = C_t$, and the dotted blue line is from eq 5, assuming a logarithmic dependence of α on the total concentration and a cmc of 29 mM. The cmc's have been obtained locally from eq 5. The dashed black straight line links the 1 M cmc data point to the 29 mM point on the line of unit slope.

most common solvent is water, but there are also many applications of micellizing systems in nonaqueous solvents.²⁵ As suggested in the Time and Length Scales section, for common surfactant molecules of practical interest at concentrations near the cmc, the vast majority of entities in solution are solvent molecules. A direct approach to the molecular modeling of such systems involves describing both surfactant and solvent with detailed atomistic models. Surfactant molecules are described either as united atom models^{26,27} or, in more recent years, using explicit-hydrogen all-atom models.^{28,29} By far the most common functional form to represent repulsion and dispersion interactions is the Lennard-Jones (12, 6) potential, with parameters obtained to match a target set of experimentally measured properties. Angle bending and torsional terms are used to capture the conformational flexibility, with parameters frequently obtained from quantum chemical calculations. For polar groups, partial charges are included in the models, from a combination of quantum chemical calculations and fitting of the experimental data. Water models in common usage³⁰ typically involve three or four sites, one of which is for the O dispersion interactions and the remainder corresponding to point fractional charges to approximate the charge distribution and hydrogen bonding interactions in real water.

There are distinct advantages in utilizing atomistically detailed, explicit-solvent models rather than coarse-grained models or the implicit-solvent models discussed in the following section. In particular, atomistically detailed models are, in principle, capable of correctly describing the local structure and can maintain a direct connection to the dynamics of the real systems. There is no need to determine effective force-field parameters to describe solvent effects, and the resulting models are more likely to be transferrable to different thermodynamic conditions of temperature or pressure or to different solvent environments.

As already stated, simulating the self-assembly of explicit-solvent dilute surfactant systems over the time scales required to reach equilibrium in dilute solutions is quite challenging. Explicit-solvent simulations are usually carried out using molecular dynamics, in other words, by numerically solving Newton's equations of motion. Typical time steps required for energy conservation and the long-term stability of simulations of atomistically detailed potentials are on the order of femtoseconds (10^{-15} s), so reaching multimicrosecond time scales involves executing more than 10^9 time steps. Moreover, atomistically detailed, explicit-solvent models cannot be combined easily with insertion (grand canonical) methods that are necessary for controlling the chemical potential of species such as added salts in the vicinity of a micellar aggregate.

Early simulations of micellar systems using atomistic, explicit-solvent models relied on preformed micellar aggregates^{31–33} with 15–60 surfactants, but more recent studies³⁴ have included larger, elongated micelles. Such simulations provide valuable insights into the internal structure of the micellar aggregates but cannot provide information on the cmc and aggregation behavior.

In recent years, several explicit-solvent simulations of spontaneous self-assembly for surfactant solutions have been attempted, with varying degrees of success with respect to reaching an equilibrium distribution of micellar aggregates. Marrink et al.³⁵ used an atomistic model of dodecylphosphocholine (DPC) in explicit water and observed the formation of

spherical or cylindrical micelles, depending on the concentration of surfactant, for run times of 10–50 ns. Sammalkorpi et al.⁸ performed 200 ns simulations of an initially randomly dispersed system of SDS surfactants in water at a concentration of 700 mM, with or without added salt. Spontaneous self-assembly was observed, and the micelles had higher aggregation numbers and were more elongated at higher salt concentrations, in agreement with experiments. However, these simulations were not sufficiently long to achieve an equilibrium distribution of micelle sizes, and no attempt was made to determine the cmc of this strongly micellizing system. Replica-exchange, constant-pH molecular dynamics simulations were used in ref 36 to investigate the self-assembly of a model titratable surfactant, and cationic–anionic surfactant mixtures were investigated in ref 37 using runs of 200 ns duration.

Equilibrium simulations of micellization can be more easily achieved for weakly micellizing surfactants. These have significantly higher cmc's than their strongly micellizing counterparts and also much faster micelle–monomer exchange and micelle restructuring dynamics. Sammalkorpi et al.³⁸ performed 200 ns atomistic molecular dynamics simulations of sodium hexyl sulfate solutions, which were shown to be long enough for full equilibration of the micelle size distribution in the salt-free and monovalent salt cases, but not for systems with added divalent salt. Measuring the free surfactant concentration in weakly micellizing systems poses challenges because of sensitivity of the aggregate size distributions to the cutoff distance used to distinguish between aggregates and monomers. The (salt-free) cmc was estimated to be between 200 and 250 mM, somewhat lower than the experimental range of 420⁷ to 517 mM.³⁹ The simulation cmc estimates were not corrected for overall surfactant concentration effects, but such effects are expected to be small in systems for which the simulated overall concentration is near the cmc.

Simulations using simplified, coarse-grained models can reach much longer time scales because they involve fewer interaction centers and can use larger time steps and also because the resulting dynamics are accelerated relative to the more detailed models.^{40–46} Zwitterionic and nonionic models within both the MARTINI framework^{47,48} and the Shinoda et al. model⁴⁹ have been studied by Sanders and Panagiotopoulos⁵⁰ using replica-exchange molecular dynamics simulations. Even though quite long runs were utilized (up to 1.8 μ s), full equilibration of the systems at room temperature was not possible, and an extrapolation of the cmc from higher temperatures had to be performed. The coarse-grained models significantly underpredict experimental cmc's near room temperature for zwitterionic surfactants but are closer to measured values for nonionic ones. The aggregation numbers for both zwitterionic and nonionic surfactants are near those observed experimentally, but the temperature dependence of the cmc is incorrect, most likely because of the use of an unstructured solvent. Results for DPC are shown in Figure 5. This study used the free surfactant concentration as a proxy for the cmc, which may result in an underestimation of the true cmc of the models, but this effect is expected to be much less severe for zwitterionic or nonionic surfactants relative to that for ionic surfactants.

The Shinoda et al. coarse-grained model for sodium alkyl sulfate surfactants⁵¹ was studied by LeBard et al.⁹ using long molecular dynamics simulations on graphics processing units (GPUs). These simulations used the efficient open-source HOOMD package⁵² with added Ewald summation capabilities.

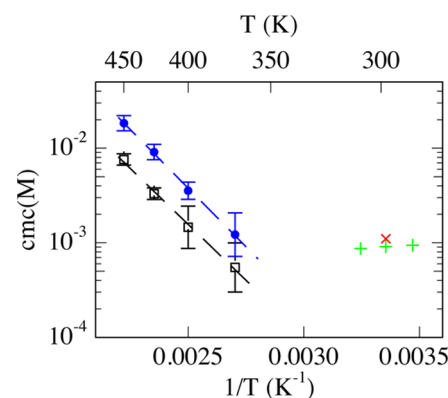


Figure 5. Critical micelle concentration versus inverse temperature for DPC.⁵⁰ Open squares are for the original MARTINI model,⁴⁷ filled circles are for MARTINI v. 2.0,⁴⁸ and dashed lines are fitted to the simulation results. Experimental values are shown as cross and plus symbols.

Approximately 0.36 ms of trajectory data was generated, allowing several independent replicas of individual systems at different chain lengths and overall surfactant concentrations to be studied over multimicrosecond time scales. The time evolution of the free surfactant concentration and size distribution of micelles for the SDS model have already been presented in Figure 2. The free surfactant concentrations for three different overall surfactant loadings are shown in Figure 6

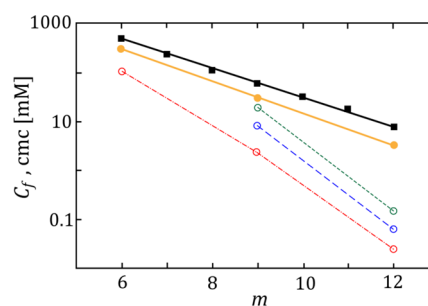


Figure 6. Free surfactant concentration, C_f , and cmc for sodium alkyl sulfate surfactants as a function of alkyl chain length m .⁹ Open symbols correspond to C_f : red open circles and dashed–dotted lines are for overall concentration $C_t = 1$ M, blue open circles and long-dashed lines are for $C_t = 363$ mM, and green open circles and dashed lines are for $C_t = 130$ mM. Solid orange circles and the line are the extrapolated cmc values using eq 2. Solid black squares and the line are experimental cmc values.

as a function of chain length m . The dependence of C_f on C_t discussed in the previous section is apparent from this plot; this dependence is less severe for lower alkyl chain lengths m because the cmc is higher, and thus concentrations used in the simulations correspond to conditions significantly closer to the cmc. The simulation-based extrapolated cmc values systematically underpredict the experimental cmc's by factors of between 2 and 3.

Sanders et al.¹² have used 400 ns molecular dynamics simulations for combinations of atomistic models of sodium alkyl sulfates of chain lengths $m = 6$ to 9 (hexyl to nonyl) with two different water models. Equation 5 was used to convert the observed free surfactant concentrations to cmc values, as already shown in Figure 4 for the case of $m = 8$. Figure 7 displays the temperature dependence of the free surfactant

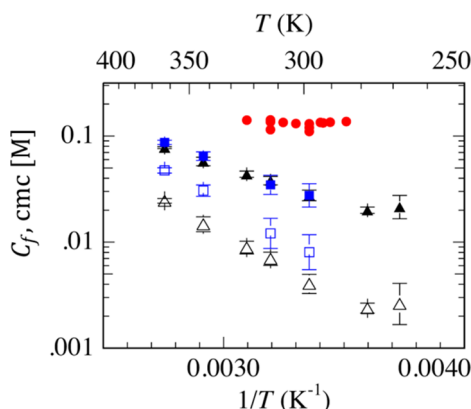


Figure 7. Temperature dependence of the cmc and free surfactant concentration, C_f , for an atomistic model of sodium octyl sulfate in explicit water.¹² C_f values from the simulations are shown as black open triangles ($C_t = 1$ M) and blue open squares ($C_t = 500$ mM). Solid symbols are cmc values: black triangles and blue squares are from simulation data at $C_t = 1$ M and 500 mM, extrapolated using eq 5; filled red circles are experimental cmc data.

concentrations and calculated cmc's, again for the case of $m = 8$. Even though the models used in ref 12 are much more detailed (and thus computationally expensive) relative to the coarse-grained models of LeBard et al.,⁹ an underestimation of the cmc values by factors of 3–5 is again observed. Moreover, the temperature dependence of the cmc is much stronger than what is observed experimentally, and the minimum in the cmc occurs at lower temperatures. These discrepancies point to deficiencies in the force fields that will need to be remedied in the future, as discussed in the last section of this article.

Even if full equilibration with respect to micelle aggregation numbers cannot yet be achieved in atomistic simulations, the results are useful for predicting the size, shape, and structure of micellar aggregates and how solutes partition between free solution and the interior of micelles, two key questions posed in the Introduction. For example, the size and shape distributions of micellar aggregates formed by sodium alkyl sulfates and the distribution of various groups with respect to the center of mass of the aggregates have been reported in detail.^{8,38} Direct observation of partitioning is not possible for most solutes of interest because the time scales for equilibration are comparable to those for monomer–micelle surfactant exchange, and the concentrations of solvophobic solutes in free solution can be quite low. Thus, an indirect method involving calculations of free energies of solutes in the interior of micelles and in free solution needs to be used. One promising path for this is to use a statistical thermodynamic model to obtain the free energy of a solute, given the atomistic structure of micelles observed in the simulations. For example, Storm et al.^{53,54} have combined atomistic simulations of pure and mixed micelles with the COSMO-RS model to obtain partitioning for a range of small molecules.

■ IMPLICIT-SOLVENT SIMULATIONS

Because micellization occurs in dilute solutions, it is natural to attempt to accelerate simulations by eliminating the solvent molecules.⁵⁵ For strongly micellizing systems, however, eliminating the solvent does not eliminate the problem of slow equilibration of quantities such as the micelle size distribution, which requires the breakup and reformation of aggregates. A preformed aggregate would not necessarily break

up if the overall surfactant concentration (or chemical potential) is below the cmc in a simulation of finite duration; conversely, micelles may not form from a solution above the cmc because the nucleation of a stable micellar nucleus is a rare event, except at concentrations much higher than the cmc. These are akin to the hysteresis problems preventing the accurate determination of phase equilibrium conditions from standard single-phase simulations. In this section, we outline a systematic methodology^{56,57} that addresses this metastability issue.

Grand canonical Monte Carlo simulations are performed in a simulation box of fixed volume, with imposed values of the temperature and chemical potential of components. Because such simulations need to include insertion and deletion steps, they are practical only for implicit-solvent models of surfactant solutions. One advantage they have over constant-particle-number simulations is that they provide the free energy of a system as a function of thermodynamic conditions, thus allowing all other properties (e.g., energy or pressure) to be computed. In the context of micellization simulations, their primary benefit is that they allow the bypassing of free-energy barriers for micelle nucleation or breakup, as shown schematically in Figure 8. In this figure, the blue ovals represent regions

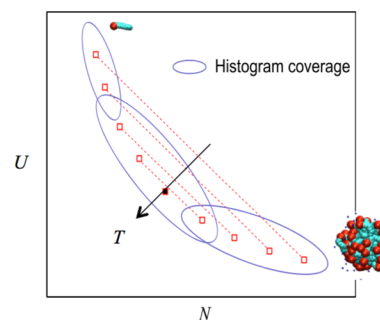


Figure 8. Schematic of the grand canonical methodology for overcoming free-energy barriers in the energy U versus number N plane.

of total energy U and the number of surfactants in the simulation box, N , sampled by a single grand canonical simulation. The red squares and dotted lines represent states of (nearly) equal free energies corresponding to the transition from free surfactants to micelles. At low temperatures, a single simulation cannot overcome the free-energy barrier for micelle formation or breakup and remains in the region from which it was initialized, either free surfactants or micelles. However, when the temperature is increased, micellization becomes weaker, and it is possible to sample the breakup and formation of micelles reversibly. By connecting regions of overlap, a free-energy surface can be constructed that can be used to model the transition. Specifically, the free energy can be used to obtain the osmotic pressure of the solution, Π , as a function of the total surfactant concentration, C_t . A typical trace of the calculated osmotic pressure curve is shown in Figure 9. At low overall surfactant concentrations, the solution is almost ideal, and the osmotic pressure curve is linear, with a slope corresponding to $\Pi = C_t k_B T$, where $C_t = N/V$ is the molar density of surfactant molecules in solution, N is the number of surfactants, and V is the volume of the simulation box. Around the cmc (marked with an arrow on Figure 9), aggregates start appearing and the osmotic pressure slope decreases significantly because the independent kinetic entities in the solution are now

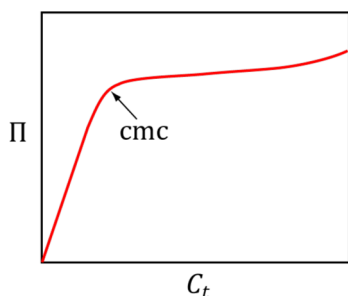


Figure 9. Schematic of osmotic pressure, Π , versus the total surfactant concentration, C_t .

aggregates of size $M \gg 1$. At even higher concentrations, micelle–micelle repulsions start appearing, and the slope increases again. The original publications^{56,57} give details on the computational methodology used to obtain cmc's in implicit-solvent models and provide applications to a simple lattice model for nonionic surfactants.⁵⁸ Because the osmotic pressure curve is obtained from histogram reweighting without any prior knowledge of micelle formation, it provides an operational definition of the cmc that does not rely on the observation of actual micelles in the simulated system. For surfactants with low cmc's in reasonable size simulation boxes, the probability of observing a micelle can be extremely low.

To apply this methodology to chemically identifiable surfactant molecules, an approach to obtaining effective potentials for the corresponding implicit-solvent models is needed. For ionic surfactants, such an approach was developed by Jusufi et al.²⁴ The approach is schematically illustrated in Figure 10. The ionic headgroups along with their counterions

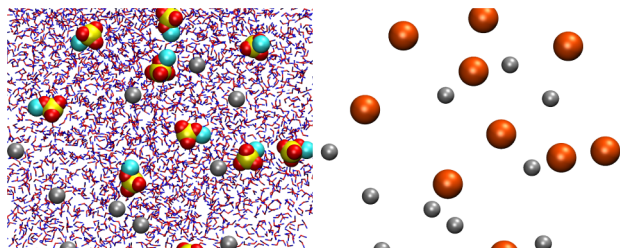


Figure 10. (Left) Atomistic simulation of SDS headgroups and counterions in explicit water. (Right) Implicit water system with coarse-grained headgroup particles (large spheres) and counterions (small spheres). Reproduced with permission from ref 24. Copyright American Chemical Society.

are first simulated in an atomistically described solvent (left panel of Figure 10). An effective potential that involves short-range hydration interactions and a distance-dependent dielectric permittivity⁵⁹ is fitted to the atomistic pair correlation functions. The resulting coarse-grained model (right panel of Figure 10) is then coupled with a standard atomistic model for the hydrocarbon tail. Solvophobic interactions of the tail group are incorporated into the model with a single attractive interaction that is placed at the end-bead of the tail, with the magnitude adjusted to match the cmc value for a specific surfactant. The transferability of this approach to surfactants of varying chain length and headgroup type was demonstrated in ref 24, and its ability to model salt effects on the cmc and the aggregation number of ionic and cationic systems was demonstrated in ref 60. Nonionic surfactants and temperature-dependent properties within this framework were

obtained in ref 61. Overall, the quality of predictions from the implicit solvent approach depends sensitively on the hydrophobic attraction parameter and the temperature functionality assumed for the implicit-solvent dielectric permittivity. Once the model has been adequately validated for a specific surfactant type, predictions for cmc's and aggregation numbers of related surfactants and surfactant mixtures become possible.

A recent application of the implicit-solvent micellization approach described in this section has been the interpretation of scattering data for dilute surfactant solutions. Scattering experiments are often used to determine the structural properties of micelles, particularly their size and shape.⁶² Because of improvements in scattering facilities, studies of dilute surfactant systems close to the cmc have become feasible.^{63,64} Molecular simulations can help to interpret properly the results obtained from small-angle X-ray scattering experiments (SAXS).⁶⁵ In this respect, implicit solvent simulations have two distinct advantages over their explicit-solvent counterparts. The first is that the cost of sampling motions of the solvent molecules is avoided. The second is that larger box lengths L can be easily used to capture the relevant range of wave vectors q . For example, SAXS experiments for tetradecyltrimethylammonium bromide (TTAB) were conducted at a concentration of 17 mM and a lower q range requiring an $L = 47.7$ nm box size.⁶⁶ Whereas explicit solvent simulations would require an additional 10^6 solvent molecules under such experimental conditions, implicit solvent modeling⁶⁵ allows us to focus solely on the solutes (total of around 17 000 particles). Figure 11 shows such a comparison between the experimental and simulated total scattering function as well as the partial intensity caused by Br^- counterions only.

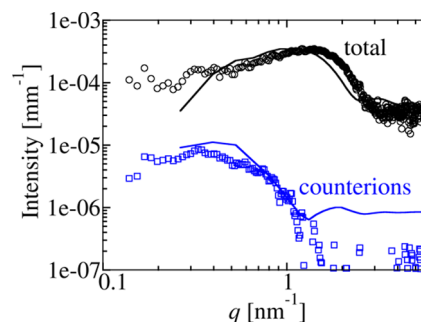


Figure 11. Scattering intensities of TTAB micelles at 17 mM. Symbols are experimental data from anomalous SAXS measurements,⁶⁶ and lines are simulation results.⁶⁵

SUMMARY AND FUTURE DIRECTIONS

Atomistic, explicit-solvent simulations can already reach time scales relevant to the micellization of weakly micellizing surfactants, provided that their cmc is not too low. However, even for surfactant molecules as simple as sodium dodecyl sulfate, the required time scales to reach full equilibration are many microseconds, currently outside the capabilities of mainstream computational facilities, and the concentrations that can realistically be simulated are orders of magnitude greater than the cmc. Because of a strong dependence of the free surfactant concentration on the overall loading in the system, careful extrapolations to lower concentrations are necessary to obtaining reliable estimates. Moreover, at high

surfactant concentrations morphological and shape transitions may also occur over long time scales, further complicating the task of extrapolation to dilute solutions.

Despite these limitations, atomistic simulations can provide useful information on the detailed structure of aggregates and dynamics of micelle formation under changing conditions of salt concentration and surfactant loading. Further development of codes optimized to take advantage of massive parallelism, coupled with hardware advances, will clearly extend the range of systems that can be studied by atomistic simulations.

An issue that remains unresolved is that highly optimized force fields that quantitatively predict water/hydrocarbon phase behavior seem to underpredict the cmc by factors of between 2 and 5. It is likely that some physical effects missing from the current models (e.g., polarizability) will need to be included before quantitative models can be obtained. The temperature dependence of properties is still a significant problem, even with atomistically detailed models.

For the many systems that remain outside the scope of atomistically detailed, explicit-solvent simulations, because of length scale and time scale limitations, coarse-grained and implicit-solvent simulations will need to be used. Both approaches sacrifice some of the broad transferability expected with fully atomistic models because their force field parameters need to be adjusted for different temperatures or solvent conditions. Coarse-grained, explicit-solvent models retain hydrodynamic interactions that can be important in non-equilibrium assembly processes,⁶⁷ and implicit-solvent simulations have the advantage that they can efficiently simulate much larger dilute surfactant systems. Nevertheless, neither coarse-grained nor implicit-solvent models preserve the true dynamics of the self-assembly process. Which model is preferable depends on the nature of the question being asked. For example, if realistic self-assembly dynamic behavior is important, then explicit-solvent models are to be preferred; by contrast, if the equilibrium behavior of low-concentration systems or the modeling of systems with high barriers to the nucleation and breakup of aggregates is of interest, then implicit-solvent models that can sample such processes have a distinct advantage.

Even though the theoretical framework for understanding the relationship between free and total surfactant concentration seems to be robust for extrapolating the behavior of ionic surfactant systems to the cmc, the corresponding relationships for nonionic surfactants have not yet been investigated in detail. There are clear indications that the free surfactant concentration also decreases above the cmc,¹¹ but the precise functional form remains to be validated against careful simulations. It is also not clear if cmc's obtained from the osmotic pressure curves in grand canonical simulations match the extrapolated cmc's from much higher concentrations in conventional (constant-volume or constant-pressure) simulations.

AUTHOR INFORMATION

Corresponding Author

*E-mail: azp@princeton.edu.

Notes

The authors declare no competing financial interest.

Biographies



Arben Jusufi received his Ph.D. in physics from Heinrich-Heine-University in Düsseldorf, Germany. He held research scientist and postdoctoral positions at the University of Bayreuth, Princeton University, and the University of Pennsylvania/Temple University. In 2011, he became an assistant professor in the chemistry department of the College of Staten Island, City University of New York. Most recently he assumed a research position at Corporate Strategic Research of ExxonMobil. His research interests are focused on the development and application of molecular modeling tools and theoretical approaches to study structure/property relationships of complex fluids.



Athanassios Z. Panagiotopoulos received an undergraduate degree from the National Technical University of Athens and a Ph.D from MIT, both in chemical engineering. After a postdoctoral position in physical chemistry at the University of Oxford, he held faculty positions at Cornell and the University of Maryland; he is currently the Susan Dod Brown Professor of Chemical and Biological Engineering at Princeton University. He is a member of the U.S. National Academy of Engineering and the American Academy of Arts and Sciences. His research interests are the development and application of theoretical and computer simulation techniques for the study of properties of fluids and materials.

ACKNOWLEDGMENTS

Our work has been supported by the Department of Energy, Office of Basic Energy Sciences, under grant DE-SC0002128. Additional support has been provided by the Princeton Center for Complex Materials (PCCM), a U.S. National Science Foundation Materials Research Science and Engineering Center (grant DMR-0819860).

REFERENCES

- (1) Jusufi, A. Molecular simulations of self-assembly processes of amphiphiles in dilute solutions: the challenge for quantitative modelling. *Mol. Phys.* **2013**, *111*, 3182–3192.
- (2) Shelley, J. C.; Shelley, M. Y. Computer simulation of surfactant solutions. *Curr. Opin. Colloid Interface Sci.* **2000**, *5*, 101–110.
- (3) Brodskaya, E. N. Computer simulations of micellar systems. *Colloid J.* **2012**, *74*, 154–171.
- (4) Israelachvili, J. *Intermolecular and Surface Forces*, 2nd ed.; Academic Press: London, 1991.
- (5) Paula, S.; Sus, W.; Tuchtenhagen, J.; Blume, A. Thermodynamics of Micelle Formation as a Function of Temperature - A High-Sensitivity Titration Calorimetry Study. *J. Phys. Chem.* **1995**, *99*, 11742–11751.
- (6) Ogino, K.; Kakahara, T.; Abe, M. Estimation of the Critical Micelle Concentrations and the Aggregation Numbers of Sodium Alkyl Sulfates by Capillary-Type Isotachopheresis. *Colloid Polym. Sci.* **1987**, *265*, 604–612.
- (7) Rassing, J.; Sams, P. J.; Wynjones, E. Kinetics of Micellization from Ultrasonic Relaxation Studies. *J. Chem. Soc., Faraday Trans. 2* **1974**, *70*, 1247–1258.
- (8) Sammalkorpi, M.; Karttunen, M.; Haataja, M. Ionic Surfactant Aggregates in Saline Solutions: Sodium Dodecyl Sulfate (SDS) in the Presence of Excess Sodium Chloride (NaCl) or Calcium Chloride (CaCl₂). *J. Phys. Chem. B* **2009**, *113*, S863–S870.
- (9) LeBard, D. N.; Levine, B. G.; Mertmann, P.; Barr, S. A.; Jusufi, A.; Sanders, S.; Klein, M. L.; Panagiotopoulos, A. Z. Self-assembly of coarse-grained ionic surfactants accelerated by graphics processing units. *Soft Matter* **2012**, *8*, 2385–2397.
- (10) Jusufi, A.; LeBard, D. N.; Levine, B. G.; Klein, M. L. Surfactant Concentration Effects on Micellar Properties. *J. Phys. Chem. B* **2012**, *116*, 987–991.
- (11) Mackie, A. D.; Panagiotopoulos, A. Z.; Szleifer, I. Aggregation behavior of a lattice model for amphiphiles. *Langmuir* **1997**, *13*, S022–S031.
- (12) Sanders, S. A.; Sammalkorpi, M.; Panagiotopoulos, A. Z. Atomistic Simulations of Micellization of Sodium Hexyl, Heptyl, Octyl, and Nonyl Sulfates. *J. Phys. Chem. B* **2012**, *116*, 2430–2437.
- (13) Gunnarsson, G.; Jönsson, B.; Wennerström, H. Surfactant association into micelles. An electrostatic approach. *J. Phys. Chem.* **1980**, *84*, 3114–3121.
- (14) Puvvada, S.; Blankschtein, D. Molecular-thermodynamic approach to predict micellization, phase behavior, and phase separation of micellar solutions. I. Application to nonionic surfactants. *J. Chem. Phys.* **1990**, *92*, 3710.
- (15) Nagarajan, R.; Ruckenstein, E. Theory of surfactant self-assembly: a predictive molecular thermodynamic approach. *Langmuir* **1991**, *7*, 2934–2969.
- (16) Blankschtein, D.; Shiloach, A.; Zoeller, N. *Curr. Opin. Colloid Interface Sci.* **1997**, *2*, 294.
- (17) Srinivasan, V.; Blankschtein, D. Effect of counterion binding on micellar solution behavior: 1. Molecular-thermodynamic theory of micellization of ionic surfactants. *Langmuir* **2003**, *19*, 9932–9945.
- (18) Maibaum, L.; Dinner, A. R.; Chandler, D. Micelle Formation and the Hydrophobic Effect. *J. Phys. Chem. B* **2004**, *108*, 6778.
- (19) Stephenson, B. C.; Goldsipe, A.; Blankschtein, D. *J. Phys. Chem. B* **2008**, *112*, 2357–2371.
- (20) Levin, Y. Electrostatic correlations: From plasma to biology. *Rep. Prog. Phys.* **2002**, *65*, 1577–1632.
- (21) Quina, F. H.; Nassar, P. M.; Bonilhaf, J. B. S.; Bales, B. L. Growth of Sodium Dodecyl Sulfate Micelles with Detergent Concentration. *J. Phys. Chem.* **1995**, *99*, 17028–17031.
- (22) Soldi, V.; Keiper, J.; Romsted, L. S.; Cuccovia, I. M.; Chaimovich, H. *Langmuir* **2000**, *16*, 59.
- (23) Bales, B. L. A Definition of the Degree of Ionization of a Micelle Based on Its Aggregation Number. *J. Phys. Chem. B* **2001**, *105*, 6798–6804.
- (24) Jusufi, A.; Hynninen, A. P.; Panagiotopoulos, A. Z. Implicit Solvent Models for Micellization of Ionic Surfactants. *J. Phys. Chem. B* **2008**, *112*, 13783–13792.
- (25) Pileni, M. P. Reverse micelles as microreactors. *J. Phys. Chem.* **1993**, *97*, 6961–6973.
- (26) Jorgensen, W. L.; Tirado-Rives, J. The OPLS [optimized potentials for liquid simulations] potential functions for proteins, energy minimizations for crystals of cyclic peptides and crambin. *J. Am. Chem. Soc.* **1988**, *110*, 1657–1666.
- (27) Martin, M. G.; Siepmann, J. I. Transferable potentials for phase equilibria. 1. United-atom description of n-alkanes. *J. Phys. Chem. B* **1998**, *102*, 2569–2577.
- (28) Jorgensen, W. L.; Maxwell, D. S.; Tirado-Rives, J. Development and Testing of the OPLS All-Atom Force Field on Conformational Energetics and Properties of Organic Liquids. *J. Am. Chem. Soc.* **1996**, *118*, 11225–11236.
- (29) Chen, B.; Siepmann, J. I. Transferable Potentials for Phase Equilibria. 3. Explicit-Hydrogen Description of Normal Alkanes. *J. Phys. Chem. B* **1999**, *103*, 5370–5379.
- (30) Vega, C.; Abascal, J. L. F. Simulating water with rigid non-polarizable models: a general perspective. *Phys. Chem. Chem. Phys.* **2011**, *13*, 19663–19688.
- (31) Jönsson, B.; Edholm, O.; Teleman, O. Molecular dynamics simulations of a sodium octanoate micelle in aqueous solution. *J. Chem. Phys.* **1986**, *85*, 2259–2271.
- (32) Watanabe, K.; Ferrario, M.; Klein, M. L. Molecular dynamics study of a sodium octanoate micelle in aqueous solution. *J. Phys. Chem.* **1988**, *92*, 819–821.
- (33) Bruce, C. D.; Berkowitz, M. L.; Perera, L.; Forbes, M. D. E. Molecular Dynamics Simulation of Sodium Dodecyl Sulfate Micelle in Water: Micellar Structural Characteristics and Counterion Distribution. *J. Phys. Chem. B* **2002**, *106*, 3788–3793.
- (34) Tang, X. M.; Koenig, P. H.; Larson, R. G. Molecular Dynamics Simulations of Sodium Dodecyl Sulfate Micelles in Water-The Effect of the Force Field. *J. Phys. Chem. B* **2014**, *118*, 3864–3880.
- (35) Marrink, S. J.; Tieleman, D. P.; Mark, A. E. Molecular dynamics simulation of the kinetics of spontaneous micelle formation. *J. Phys. Chem. B* **2000**, *104*, 12165–12173.
- (36) Morrow, B. H.; Koenig, P. H.; Shen, J. K. Self-Assembly and Bilayer-Micelle Transition of Fatty Acids Studied by Replica-Exchange Constant pH Molecular Dynamics. *Langmuir* **2013**, *29*, 14823–14830.
- (37) Chen, J. F.; Hao, J. C. Molecular dynamics simulation of cetyltrimethylammonium bromide and sodium octyl sulfate mixtures: aggregate shape and local surfactant distribution. *Phys. Chem. Chem. Phys.* **2013**, *15*, 5563–5571.
- (38) Sammalkorpi, M.; Sanders, S.; Panagiotopoulos, A. Z.; Karttunen, M.; Haataja, M. Simulations of Micellization of Sodium Hexyl Sulfate. *J. Phys. Chem. B* **2011**, *115*, 1403–1410.
- (39) Suarez, M. J.; Lopez-Fontan, J. L.; Sarmiento, F.; Mosquera, V. Thermodynamic study of the aggregation behavior of sodium n-hexyl sulfate in aqueous solution. *Langmuir* **1999**, *15*, S265–S270.
- (40) Velinova, M.; Sengupta, D.; Tadjer, A. V.; Marrink, S. J. Sphere-to-Rod Transitions of Nonionic Surfactant Micelles in Aqueous Solution Modeled by Molecular Dynamics Simulations. *Langmuir* **2011**, *27*, 14071–14077.
- (41) Sangwai, A. V.; Sureshkumar, R. Coarse-Grained Molecular Dynamics Simulations of the Sphere to Rod Transition in Surfactant Micelles. *Langmuir* **2011**, *27*, 6628–6638.
- (42) Kraft, J. F.; Vestergaard, M.; Schiott, B.; Thøgersen, L. Modeling the Self-Assembly and Stability of DHPC Micelles Using Atomic Resolution and Coarse Grained MD Simulations. *J. Chem. Theory Comput.* **2012**, *8*, 1556–1569.
- (43) Vishnyakov, A.; Lee, M. T.; Neimark, A. V. Prediction of the Critical Micelle Concentration of Nonionic Surfactants by Dissipative Particle Dynamics Simulations. *J. Phys. Chem. Lett.* **2013**, *4*, 797–802.
- (44) Lee, M. T.; Vishnyakov, A.; Neimark, A. V. Calculations of Critical Micelle Concentration by Dissipative Particle Dynamics Simulations: The Role of Chain Rigidity. *J. Phys. Chem. B* **2013**, *117*, 10304–10310.

- (45) Perez-Sanchez, G.; Gomes, J. R. B.; Jorge, M. Modeling Self-Assembly of Silica/Surfactant Mesosstructures in the Templated Synthesis of Nanoporous Solids. *Langmuir* **2013**, *29*, 2387–2396.
- (46) Marrink, S. J.; Tieleman, D. P. Perspective on the Martini model. *Chem. Soc. Rev.* **2013**, *42*, 6801–6822.
- (47) Marrink, S. J.; de Vries, A. H.; Mark, A. E. Coarse grained model for semiquantitative lipid simulations. *J. Phys. Chem. B* **2004**, *108*, 750–760.
- (48) Marrink, S. J.; Risselada, H. J.; Yefimov, S.; Tieleman, D. P.; de Vries, A. H. The MARTINI force field: Coarse grained model for biomolecular simulations. *J. Phys. Chem. B* **2007**, *111*, 7812–7824.
- (49) Shinoda, W.; DeVane, R.; Klein, M. L. Coarse-grained molecular modeling of non-ionic surfactant self-assembly. *Soft Matter* **2008**, *4*, 2454–2462.
- (50) Sanders, S. A.; Panagiotopoulos, A. Z. Micellization behavior of coarse grained surfactant models. *J. Chem. Phys.* **2010**, *132*.
- (51) Shinoda, W.; DeVane, R.; Klein, M. L. Coarse-grained force field for ionic surfactants. *Soft Matter* **2011**, *7*, 6178–6186.
- (52) Anderson, J. A.; Lorenz, C. D.; Travesset, A. General purpose molecular dynamics simulations fully implemented on graphics processing units. *J. Comput. Phys.* **2008**, *227*, 5342–5359.
- (53) Storm, S.; Jakobtorweihen, S.; Smirnova, I.; Panagiotopoulos, A. Z. Molecular Dynamics Simulation of SDS and CTAB Micellization and Prediction of Partition Equilibria with COSMOmic. *Langmuir* **2013**, *29*, 11582–11592.
- (54) Storm, S.; Jakobtorweihen, S.; Smirnova, I. Solubilization in Mixed Micelles Studied by Molecular Dynamics Simulations and COSMOmic. *J. Phys. Chem. B* **2014**, *118*, 3593–3604.
- (55) Morisada, S.; Shinto, H. Implicit Solvent Model Simulations of Surfactant Self-Assembly in Aqueous Solutions. *J. Phys. Chem. B* **2010**, *114*, 6337–6343.
- (56) Floriano, M. A.; Caponetti, E.; Panagiotopoulos, A. Z. Micellization in model surfactant systems. *Langmuir* **1999**, *15*, 3143–3151.
- (57) Panagiotopoulos, A. Z.; Floriano, M. A.; Kumar, S. K. Micellization and phase separation of diblock and triblock model surfactants. *Langmuir* **2002**, *18*, 2940–2948.
- (58) Larson, R. G. Monte-Carlo Lattice Simulation of Amphiphilic Systems in 2 and 3 Dimensions. *J. Chem. Phys.* **1988**, *89*, 1642–1650.
- (59) Lenart, P. J.; Jusufi, A.; Panagiotopoulos, A. Z. Effective potentials for 1:1 electrolyte solutions incorporating dielectric saturation and repulsive hydration. *J. Chem. Phys.* **2007**, *126*, 044509.
- (60) Jusufi, A.; Hynninen, A. P.; Haataja, M.; Panagiotopoulos, A. Z. Electrostatic Screening and Charge Correlation Effects in Micellization of Ionic Surfactants. *J. Phys. Chem. B* **2009**, *113*, 6314–6320.
- (61) Jusufi, A.; Sanders, S.; Klein, M. L.; Panagiotopoulos, A. Z. Implicit-Solvent Models for Micellization: Nonionic Surfactants and Temperature-Dependent Properties. *J. Phys. Chem. B* **2011**, *115*, 990–1001.
- (62) Pedersen, J. S. Small-Angle Scattering from Surfactants and Block Copolymer Micelles. In *Soft Matter Characterization*; Borsali, R., Pecora, R., Eds.; Springer: Heidelberg, Germany, 2008; Vol. 1, p 191.
- (63) Gummel, J.; Sztucki, M.; Narayanan, T.; Gradzielski, M. Concentration Dependent Pathways in Spontaneous Self-Assembly of Unilamellar Vesicles. *Soft Matter* **2011**, *7*, 5731.
- (64) Sztucki, M.; Di Cola, E.; Narayanan, T. Anomalous Small-Angle X-ray Scattering from Charged Soft Matter. *Eur. Phys. J.: Spec. Top.* **2012**, *208*, 319.
- (65) Jusufi, A.; Kohlmeyer, A.; Sztucki, M.; Narayanan, T.; Ballauff, M. Self-Assembly of Charged Surfactants: Full Comparison of Molecular Simulations and Scattering Experiments. *Langmuir* **2012**, *28*, 17632–17641.
- (66) Sztucki, M.; Di Cola, E.; Narayanan, T. Instrumental Developments for Anomalous Small-Angle X-ray Scattering from Soft Matter Systems. *J. Appl. Crystallogr.* **2010**, *43*, 1479.
- (67) Spaeth, J. R.; Kevrekidis, I. G.; Panagiotopoulos, A. Z. A comparison of implicit- and explicit-solvent simulations of self-assembly in block copolymer and solute systems. *J. Chem. Phys.* **2011**, *134*, 164902.